Novel Nitrogen-Containing Epoxy Resin. II. Cure Kinetics by Differential Scanning Calorimetry

Xing Hong Zhang, Yu Qin Min, Hui Zhao, Hong Mei Wan, Guo Rong Qi

Institute of Polymer Science, Zhejiang University, Hangzhou 310027, China

ABSTRACT: The isothermal and nonisothermal cure behaviors of a novel nitrogen-containing epoxy resin (XT resin) were studied by differential scanning calorimetry (DSC). Various kinetic parameters and details of cure process were obtained based on the Avrami theory. The results indicated that Avrami method is suitable for calculating the kinetic parameters up to the gel point at least. The apparent activation energy (E_a) for isothermal cure process was in agreement with that for nonisothermal cure process. E_a value in the early stage (78.5–81.0 KJ mol^{-1}) was about three times than that in the later stage (23.3–26.5 KJ mol^{-1}). The kinetic results from Avrami theory may present a combined effect of all factors, and which is helpful to understand the cure technique for XT–DDS system. © 2006 Wiley Periodicals, Inc. J Appl Polym Sci 100: 3483–3489, 2006

Key words: epoxy; cure kinetics; differential scanning calorimeter; Avrami theory

INTRODUCTION

Epoxy resins are used in many industrial applications because of their great versatility, low shrinkage, good chemical resistance, outstanding adhesion, and high-grade electrical insulation.[1] Epoxy resins cannot meet the requirement of the electronic/electrical industry unless their disadvantages such as brittleness and flammability are minimized. Generally, there are two ways to improve the properties of epoxy resins for electronic/electrical industry: synthesis of new epoxy compounds that have thermal- and flame-resistant structure; and improvement of cure techniques, which have great influences on the properties of the cured epoxy and this demands the knowledge of cure kinetics.

Compared to halogen- or phosphorus-containing flame retardants for epoxy resins,[2–9] nitrogen-containing flame-retardants such as melamine-phenol-formaldehyde novolac (MPN) resin,[10] amino isocyanurate[11] are gradually attracting a lot of attention because they are environmentally friendly with less toxicity, no dioxin, and low evolution of smoke during combustion. Much effort was made to prepare new nitrogen-containing epoxy systems for electronic/electrical products. We had reported a nitrogen-containing epoxy compound (XT resin) through chain extension between triglycidyl isocyanurate (TGIC) and xylenephenolformaldehyde (XPF resin).[11] Thermal stability, self-extinguishments, dissolvability, and hydrophobic nature of the products would be improved by the introduction of triazine structure and the unsymmetrical xylene structure.

The synthetic kinetics of XT resin was intensively investigated in our previous work[12] by GPC method. The objective of the present study was to investigate the cure kinetics of XT resin with 4, 4'-diaminodiphenylsulfone (DDS). A phenomenological model based on the Avrami theory was chosen to evaluate the cure behavior of XT–DDS system because the structure of XT resin is so complex (unsymmetrical structure, different numbers of epoxy rings in different molecular structures).

EXPERIMENTAL

Materials

Xyleneformaldehyde resin (XF2602, from Suzhou Special Chemical Co. Ltd, China): acid value < 0.3 mg KOH/g, M_w = 300–500, Oxygen content is 11 wt % (from Elemental Analysis). Triglycidyl isocyanurate (TGIC), 4, 4'-diaminodiphenylsulfone (DDS) and phenol were used as received. *p*-Toluenesulfonic acid (*p*-TSA) and lithium hydroxide were of reagent grade and used as catalysts for two reactions respectively. All solvents were commercially available and used as received, unless otherwise noted.

Preparation of XT resin

A general synthetic route (Scheme 1) of XT resin was described as the published procedures.[12] The epoxy

---
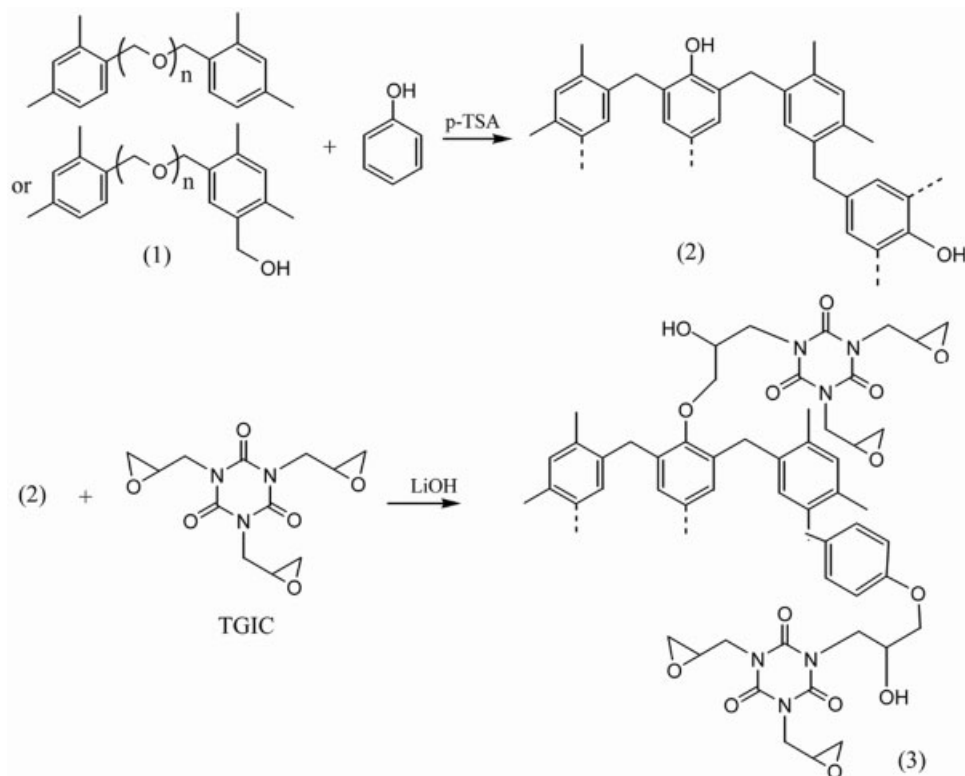
Scheme 1 Syntheses of XPF and XT resins. (1) XF resin; (2) XPF resin; (3) Ideal structure of XT resin.

equivalent weight (EEW) of XT resin was 0.28 mol/ 100 g determined by hydrochloric acid–acetone method.

DSC characterization

XT resin and DDS were dissolved in DMF separately, and then mixed homogeneously in a 1 : 1 equivalent ratio, precipitated in CH_3OH/H_2O (50/50 volume ratio). The precipitate was collected by filtration and the solvent was evaporated in vacuum in room temperature (~20°C), and then kept in a refrigerator for DSC test.

Samples consisting of 3.0–5.0 mg mixtures were placed in aluminum DSC pans and run on a PerkinElmer DSC 7 thermal analyzer. Dynamic scans were conducted at heating rates of 10, 15, 20, and 30°C min^{-1}, and were used to determine the heat relating to the cure process and kinetics. The carrier gas was nitrogen at a flow rate of 40 mL min^{-1}.

Isothermal scanning were performed over cure temperatures between 120 and 160°C in 10°C increments. After all the isothermal curing, a dynamic scan was conducted from 30°C to 300°C (15°C min^{-1}) to determine the residual heat.

The DSC curves were analyzed on the basis of the following assumptions: the area under the curves is proportional to the extent of reaction α, and the extent of reaction during the mixing of XT resin and DDS may be neglected. The extent of the cure α at any time is defined as:

$$\alpha = \frac{\Delta H_t}{\Delta H_0} \tag{1}$$

where ΔH_t is the heat of reaction determined from the partial area under DSC curve up to the point of interest, ΔH_0 is the ultimate heat of cure.

RESULTS AND DISCUSSION

Reaction extent in isothermal and nonisothermal cure process

Typical dynamic DSC curves at four heating rates (10, 15, 20, and 30°C min^{-1}) for XT–DDS system are shown in Figure 1. It is seen that the cure exotherm shift to higher temperatures with increasing heating rate. The temperature at which the maximum conversion rate occurs in the DSC curve (T_p) at different heating rates has a good linear correlation (the linear relation coefficient is 0.98). The value of reaction heat (ΔH_0) at different heating rates varied from 187 J g^{-1} to 209 J g^{-1}, might be a result of the chemical nature of XT–DDS system. The extent of cure could be calculated by
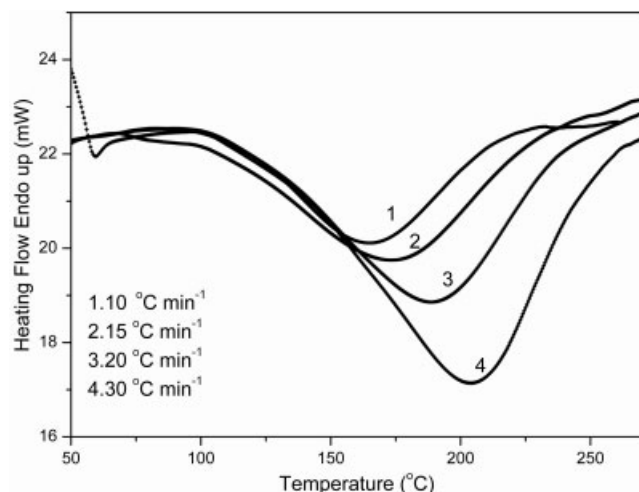
Figure 1   Dynamic DSC curves at different heating rates for XT–DDS system.

Figure 3   DSC exotherm curves for XT–DDS system at different temperatures.

eq. (1) from the curing heat (ΔH_t) which is related to the area under the exotherm.

Figure 2 shows that temperature dependence of the uncured fraction $1-\alpha$ at different heating rates for XT–DDS system and reveals that the extent of cure decreases correspondingly at the given temperature when the heating rates are increased.

Typical isothermal DSC exotherm curves for XT–DDS system at different temperatures are shown in Figure 3. And a second scanning exotherm at a heating rate of 15°C min^{-1} (Fig. 4) indicates that samples cured in low temperatures (120, 130, and 140°C) were not complete obviously. However, the corresponding residual heat of reaction by second dynamic scanning cannot be determined precisely, so we chose the value 209.3 J g^{-1} obtained from dynamic cure process as the total heat. Figure 5 shows the plot of the unreacted
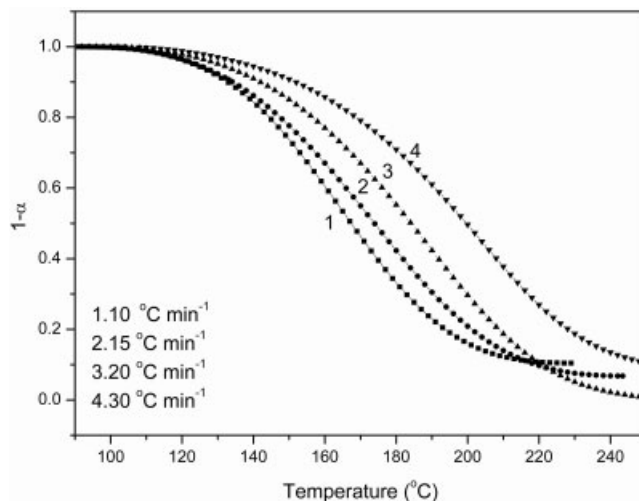
fraction $1-\alpha$ against reaction time t in the isothermal cure process. It is seen that the reaction rate and the ultimate reaction extent increase with increasing reaction temperature. The maximum cure extent is ~0.8 at 160°C. The differences of α at different temperatures in the isothermal cure process mean that the nature of the reaction and the final products may differ at different temperatures.

Isothermal kinetic analysis

It is well known that the reaction of epoxy resin with diamine is a three-dimensional polymerization. The increment of molecular weight in three-dimensional directions shows that this polymerization is not limited to chemical crosslinking and that the relationship between initial oligmer and resulting polymer structure and properties is not so straightforward as it

Figure 2   Plots of the uncured fraction $1-\alpha$ versus temperature at different heating rates for XT–DDS system.

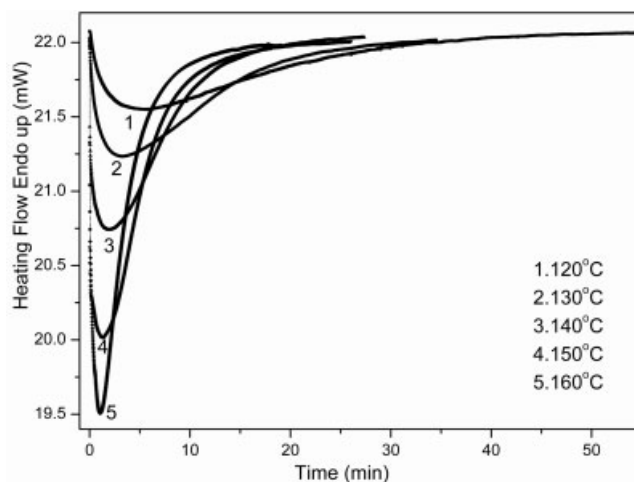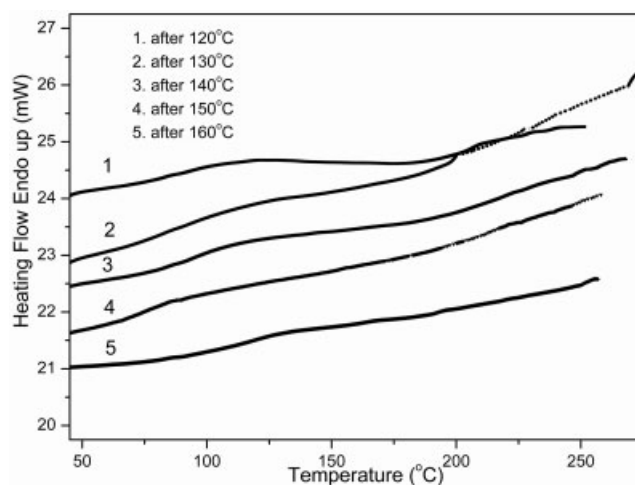**Figure 4**   The second scanning DSC curves after corresponding isothermal cure process.
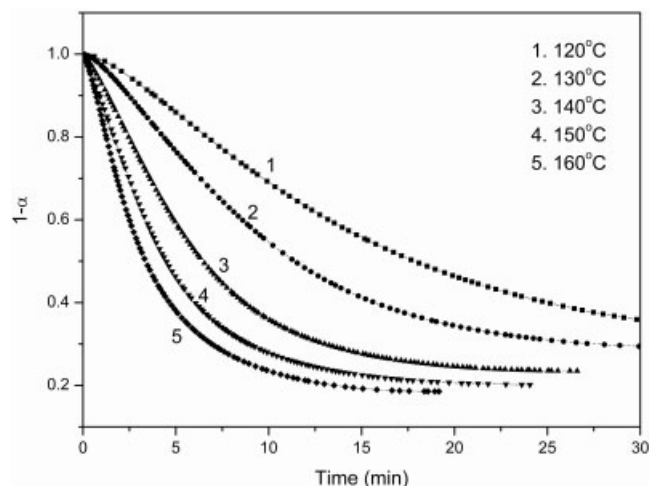
Figure 5 Plots of the uncured fraction $1-\alpha$ versus reaction time at various temperatures for XT–DDS system.

might appear.[13] In many instances,[14,15] this process is accompanied by physical and structural changes such as micro-phase separation, vitrification of the reaction medium, as well as heterogeneous polymer network formation. These changes in turn often significantly affect both polymerization kinetics and the structure and properties of the resulting polymer. Based on the above knowledge, Avrami theory could be used to describe the cure process and kinetics of epoxy–diamine systems.[16] Moreover, mechanism model requires an assumption on reaction order, which is difficult to make certain for XT–DDS system due to its complex molecular structure.

The advantage of isothermal cure process is that the rate constants at each temperature are better defined and constants at different temperatures permit determination of the activation energy associated with the cure reactions. For the isothermal cure process, the Avrami equation is:

$$1 - a = \exp(-kt^n) \qquad (2)$$

where α is the extent of cure at time t, k is the Avrami rate constant, and n is the Avrami exponent. It is well known that n provides qualitative information about the nature of the nucleation and growth process in the crystallization of a polymer. In fact, n often decreases as nucleation stops, and only the growth of nuclei continues in the later stage of the reaction kinetics. A straight line is obtained from eq. (3) when $\ln[-\ln(1-\alpha)]$ is plotted versus $\ln t$, from which n can be obtained as the slope and $\ln k$ as the intercept.

$$\ln[-\ln(1 - \alpha)] = \ln k + n \ln t \qquad (3)$$

As can be seen from Figure 6, the Avrami plots show good linearity in the early stage but a gradual

transition in slopes occur in the later stage of cure process. If there is no consideration of this gradual change, the linear relation coefficients of all data points in every temperature in Figure 6 were 0.97–0.98, which might be regarded as a good fit. But this transition indicates a gradual change in cure mechanism since the slope of the plot is a measure of the Avrami exponent n according to Avrami theory. The starting transition point was regarded as the beginning of gelation.[17] These indicate that Avrami theory could describe the cure process up to the beginning of transition, which was often regarded as the gel point.[16]

The gradual decrease of n value in the later stage implies that formation of microgels (like nucleation in crystallization of a polymer) was replaced by growth of microgels (diffusion-controlled reaction) in the advance of curing. It is reasonable to consider that the early curing process as a three-dimensional growth by instantaneous nucleation from the reaction of XT and DDS is so rapid in homogeneous medium. As the reaction proceeds, the number of microgels increases and becomes densely distributed, and they are forced to impinge on each other and the diffusion-controlled reaction becomes dominated because of a marked increase in viscosity and gelation occurred. The phase of the curing system has remarkable changes from homogeneous state to heterogeneous state and in turn these physical changes significantly affect cure kinetics.

The Avrami plots in Figure 6 can be plotted out of two differentiated sections roughly, since they are not straight lines over whole curing time. The kinetic parameters can be determined by assuming Arrhenius-type dependence for the reaction constant, i.e.

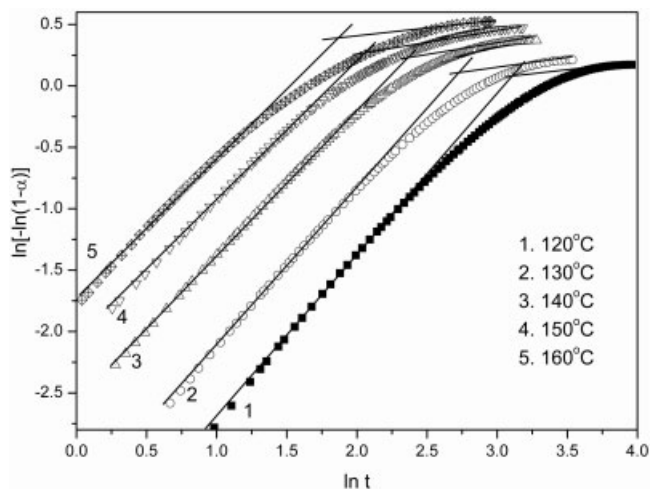$$\ln k = -\frac{E_a}{RT} + \ln A \qquad (4)$$

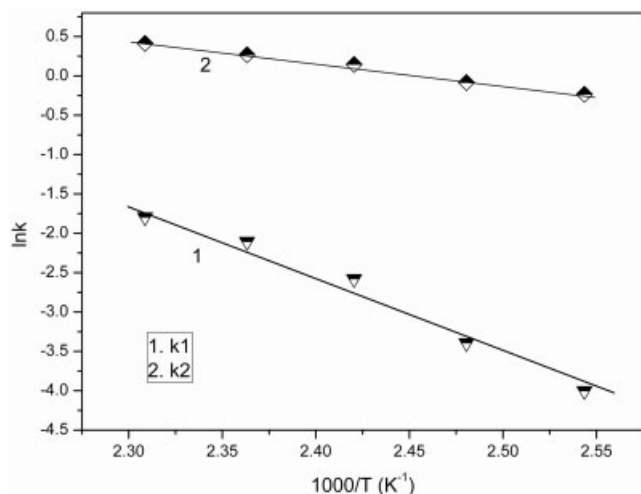**Figure 6** Avrami plots of XT–DDS system at various temperatures.

Figure 7 Arrhenius plots of rate constant for XT–DDS system in the whole cure process. Line 1: the early stage; Line 2: the later stage.

Figure 8 Avrami plots of dynamic cure of XT–DDS system at various temperatures.

where E_a is the activation energy, A is an overall frequency factor, and R is the universal gas constant.

Figure 7 shows the good linear relationship between the ln k and $1/T$ in the early and later stage. It gives a slope in which apparent activation energy is evolved. Activation energy in the early and later stage is 81.0 KJ mol^{-1} and 23.3 KJ mol^{-1} respectively.

Nonisothermal kinetics analysis

It is well known that the limitation of isothermal cure process by DSC experiment is that the nature of the reaction and the final products may differ at different temperatures.[18] Dynamic experiment at a certain heating rate by DSC experiment yield conversion–time–temperature data that are comprehensive enough to permit direct evaluations of the kinetic parameters.

In comparison with the results of the isothermal method, multiple exotherms from different heating rates are obtained. Equation (2) describes the isothermal cure process and can be extended to the dynamic process.

Here, the Ozawa method is adopted to describe the cure process of XT–DDS system at a constant heating rate.[19] At a given temperature, n is constant, the untransformed volume fraction can be written as:

$$1 - \alpha = \exp(-k'\varphi^{-n}) \tag{5}$$

where α is a function of temperature, φ is the heating rate, k' is a function of the temperature of the process. So the modified Avrami equation is:

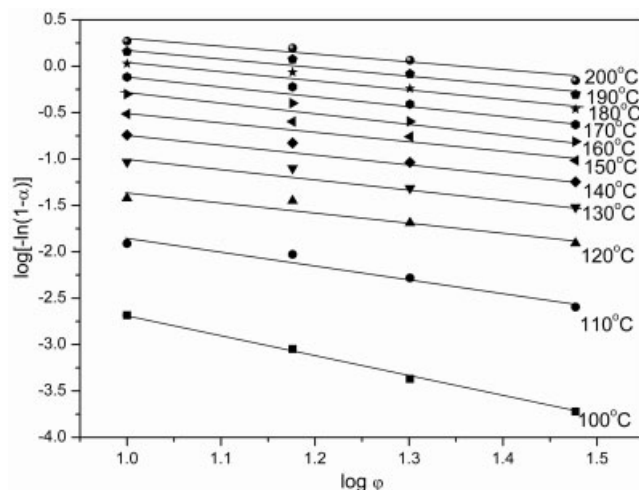$$\log[-\ln(1-\alpha)] = \log k' - n \log \varphi \tag{6}$$

A plot of $\log[-\ln(1-\alpha)]$ versus $\log \varphi$ at a given temperature should yield a straight line with a slope of $-n$ and an intercept of $\log k'$. So we can obtain the kinetic parameters from the observation of the cure process at different heating rates.

The plots in Figure 8 exhibit a good linearity in the temperature range of 100–200°C for the dynamic cure behavior of XT–DDS system. We obtain the slope $-n$ and the intercept $\log k'$. The kinetic parameters E_a is calculated by Arrhenius equation [eq. (4)].

Figure 9 depicts a plot of ln k' versus $1/T$. It can be seen that the Arrhenius plots are not straight for the whole cure temperature, but display an obvious transition in slope at around 170°C. If Arrhenius theory is obeyed at all cure process, that is, we consider no change in the slope of the lines (line 1 in Fig. 9) and
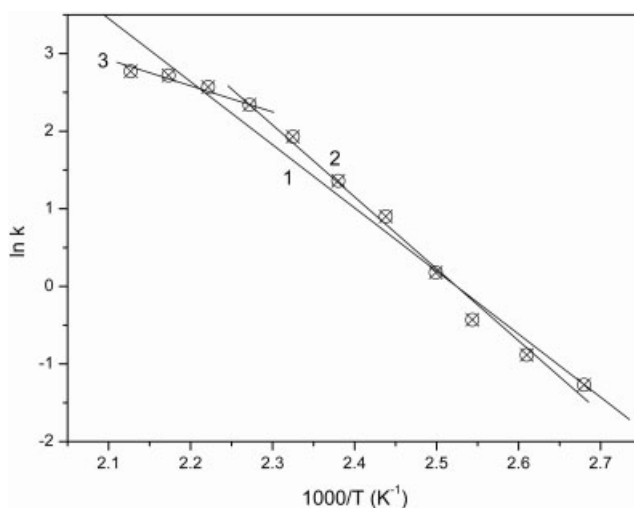

Figure 9 Temperature dependence of rate constant for XT–DDS system. 1: entire process, 2: the early, and 3: the later reaction stage.
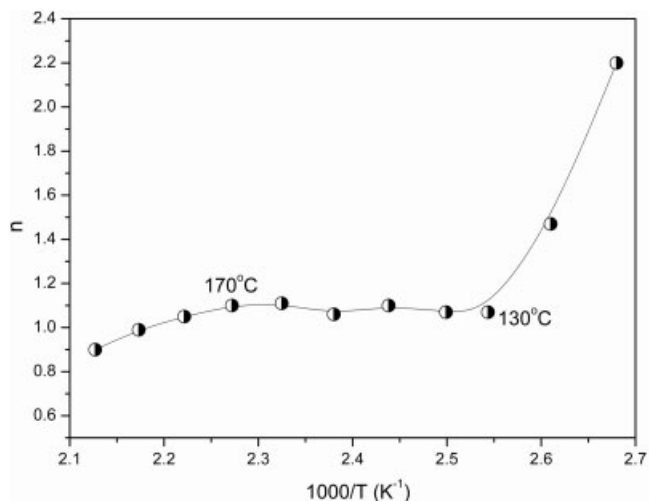
Figure 10 The curve of Avrami exponent n versus $1/T$ for XT–DDS system.

only give an overall activation energy, which is about 67.6 KJ mol^{-1} and is in agreement with other epoxy-amine systems.[20] Since the slope of the plot of ln k' versus $1/T$ is a measurement of the activation energy, the transition of the slope means a marked change in the activation energy, that is, the mechanism dominated the polymerization has a marked change. Thus we separate the whole cure process into two parts from 170°C: the early stage (before 170°C, Fig. 9 line 2) and the later stage (after 170°C, Fig. 9 line 3), and corresponding activation energy E_a is 78.5 KJ mol^{-1} and 26.5 KJ mol^{-1} respectively, based on the Arrhenius theory. The activation energies in the early and later temperature range are in good agreement with those observed in isothermal cure process (about 81.0 KJ mol^{-1} and 23.3 KJ mol^{-1}).

From above results, one can see E_a of the later stage falls to approximately one-third of the value in the early range in dynamic cure process, as the case of isothermal cure process. Such a decrease in activation energy is commonly observed in heterogeneous reactions, especially when diffusion-controlled reaction occurs.[21] Therefore, the present results may be interpreted to imply that diffusion factors become significant in the later stage of the cure process.

Figure 10 shows the nonlinear relationship of Avrami exponent n and $1/T$ in dynamic cure process for the XT–DDS system. One can see that n decreases rapidly before 130°C, and then has no obvious changes between 130°C and 170°C, and then decreases slightly after 170°C with increasing cure temperature. Before 130°C, small quantities of liquid reactants were transformed into microgels that dispersed in the solution of unreacted epoxy and DDS or prepolymer by kinetic-controlled reaction. Once the microgels formed, they would grow. The growth of microgels (reaction in the interface between microgel and solu-

tion) and the crosslinking reactions in the interior of microgels are mainly diffusion-controlled reaction that resulted in the decrease of n. When the cure temperature is in the range of 130–170°C, microgels become more "rigid" by crosslinking reaction in the interior and "bigger" by the reaction in the interface between microgel and solution. At the same time, new microgels produced continuously by kinetic-controlled reaction. Kinetic-controlled and diffusion-controlled reaction dominated the reaction in this stage, but influence of kinetic-controlled reaction on the cure decreased sharply with increasing of the viscosity of the system. With the growth of macrogels, they were impinged, and then phase conversion set in, the corresponding cure temperature is about 170°C that is the marked change in the plots of ln k versus $1/T$, and microgels were difficult to form after this temperature. Diffusion-controlled reaction was dominated thoroughly after 170°C and n decreased continuously. It is noted that the nonlinearity of Avrami exponent n and $1/T$ shows that phase conversion may occur in the cure process of the XT–DDS system and in turn significantly affect polymerization kinetics. Furthermore, the transition of kinetic-controlled reaction into diffusion-controlled reaction is gradual in the cure process and is companied with the phase conversion; there are no obvious limitations in two reaction mechanisms.

From the analysis of E_a and n, one can see the use of eq. (3) might be appropriate only when growth is completed. That is, the Avrami equation is suitable for XT–DDS system up to the gel point. And this is consistent with the conclusion of Lu et al.[16]

Kissinger method[22] was often applied to calculate E_a because it is a very simple way to deal with the dynamic cure process of epoxy–amine system. The kinetic parameters obtained from Kissinger method have no relation to the heating rate, side reactions as well as the choice of baseline.

The kissinger expression gives:

$$-\ln\left(\frac{\varphi}{T_p^2}\right) = \frac{\Delta E}{R}\frac{1}{T_p} - \ln\frac{AR}{\Delta E} \qquad (7)$$

where T_p is the temperature at which the maximum conversion rate occurs in the DSC curve, A is an overall frequency factor, and R is the universal gas constant. The activation energy values obtained from the slopes of the $-\ln(\varphi/T_p^2)$ versus $1/T_p$ plots for XT–DDS system (Fig. 11) is about 46.9 KJ mol^{-1}, which is lesser than the value from dynamic cure process according Avrami method, this might result from the different assumptions of both methods.

CONCLUSIONS

In this work, the isothermal and nonisothermal cure behaviors for XT–DDS system are studied by DSC for
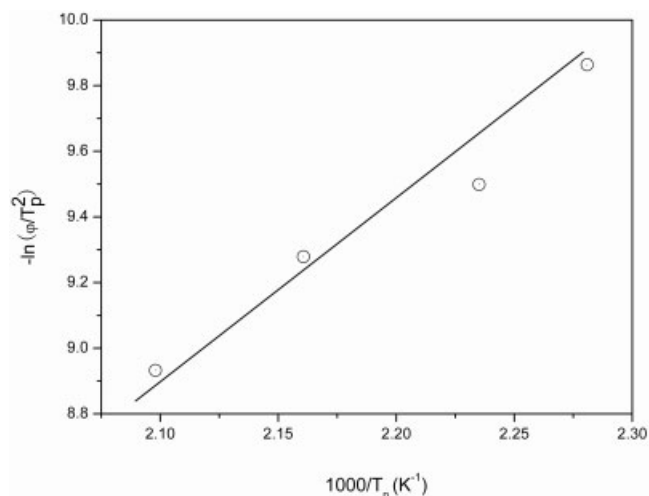
Figure 11 Plot of $-\ln(\varphi/T_p^2)$ versus $1/T_p$ for XT–DDS system.

the knowledge of cure technique. Various kinetic parameters and details of cure process were obtained based on the Avrami theory. The activation energy in the early and later stage of cure process is about 81.0 and 23.3 KJ mol^{-1} (isothermal results) and 78.5 and 26.5 KJ mol^{-1} (nonisothermal results) respectively, and agreed very well. Such a decrease in activation energy is commonly observed in heterogeneous reactions, especially when diffusion-controlled reaction occurs (after gelation). Furthermore, the nonlinear relationship of Avrami exponent n and cure temperature in isothermal and nonisothermal cure process also disclosed that phase change (from homogeneous phase to heterogeneous phase) would occur and in

turn influenced on the cure kinetics greatly. The kinetic results from Avrami theory may present a combined effect of all factors, which are helpful to understand the cure technique for XT–DDS system.

References

1. Kinjo, N.; Ogata, M.; Kaneda, A. Adv Polym Sci 1989, 88, 1.
2. Luijk, P. H.; Govers, A.; Eijkel, G. B.; Boon, J. J. J Anal Appl Pyrolysis 1991, 20, 303.
3. Cheng, K. C.; Yu, S. Y.; Chiu, W. Y. J Appl Polym Sci 2002, 83, 2733.
4. Cheng, K. C.; Yu, S. Y.; Chiu, W. Y. J Appl Polym Sci 2002, 83, 2741.
5. Liu, Y. L. Polymer 2001, 42, 3445.
6. Liu, Y. L.; Wu, C. S.; Hsu, K. Y. J Polym Sci Part A: Polym Chem 2002, 40, 2329.
7. Jain, P.; Choudhary, V.; Varma, I. K. J Appl Polym Sci 2002, 84, 2235.
8. Jeng, R. J.; Shau, S. M.; Lin, J. J.; Su, W. C. Eur Polym J 2002, 38, 683.
9. Wu, C. S.; Liu, Y. L.; Chiu, Y. C.; Chiu, Y. S. Polym Degrad Stab 2002, 78, 41.
10. Shieh, J. Y.; Wang, C. S. Polymer 2001, 42, 7617.
11. Von, G. W.; Huber, J.; Kapitza, H.; Rogler, W. J Vinyl Addit Technol 1997, 3, 175.
12. Zhang, X. H.; Wan, H. M.; Min, Y. Q.; Qi, G. R. J Appl Polym Sci 2005, 96, 723.
13. Berlin, A. A.; Matveyeva, N. G. Macromol Rev 1977, 12, 1.
14. Zhu, S.; Hamielec, A. E. Makromol Chem Macromol Symp 1993, 63, 135.
15. Liu, S. B.; Liu, J. L.; Yu, T. L. J Appl Polym Sci 1994, 53, 1165.
16. Lu, M. G.; Shim, M. J.; Kim, S. W. J Therm Anal Calorim 1999, 58, 701.
17. Pollard, M.; Karelos, J. L. Polym Eng Sci 1987, 27, 829.
18. Lee, J. Y.; Shim, M. J.; Kim, S. W. Mater Chem Phys 1997, 48, 36.
19. Ozawa, T. Polymer 1971, 12, 150.
20. Kim, S. W.; Lu, M. G.; Shim, M. J. Polym J 1998, 2, 90.
21. Desio, G. P.; Rebenfeld, L. J Appl Polym Sci 1992, 45, 2005.
22. Kissinger, B. H. Anal Chem 1957, 21, 1702.